Theoretical investigation of size and shape effects on the melting temperature and energy bandgap of TiO_2 nanostructures

G. Guisbiers,[1,a] O. Van Overschelde,[2] and M. Wautelet[2]
[1]*CICECO, University of Aveiro, Campus Santiago, 3810-193 Aveiro, Portugal*
[2]*Physics of Condensed Matter, University of Mons-Hainaut, 23 Avenue Maistriau, 7000 Mons, Belgium*

(Received 24 January 2008; accepted 22 February 2008; published online 13 March 2008)

In this letter, we report a theoretical investigation concerning the size effect on the melting temperature and energy bandgap of TiO_2 nanostructures. Within the thermodynamical approach, we predict a structural phase transition from rutile to anatase for the sizes around 40, 29, and 48 nm, respectively, in the cases of spherical nanoparticles, cylindrical nanowires, and nanotubes. For spherical nanoparticles, this means that the more stable phase is anatase for sizes smaller than ~40 nm and rutile for sizes larger than ~40 nm. The energy bandgap of these structures is also estimated. © *2008 American Institute of Physics*. [DOI: 10.1063/1.2897297]

Titanium dioxide (TiO_2) has been extensively studied in the past decades due to its interesting electric, optical, and catalytic properties.[1] It is used in diverse applications such as heterogeneous catalysis, photocatalysis, solar cells, gas sensors, white pigments, corrosion protective coating, and optical coating. TiO_2 has three different structural phases: rutile, anatase, and brookite. These phases have different thermal and optical properties. The phase is the most critical parameter determining the use of TiO_2. The rutile phase is thermally the most stable at the macroscale. The anatase phase is the most photoactive. In this letter, we propose to study the size effect on the thermal stability, melting temperature, and energy bandgap for these phases.

Since the pioneering work of Pawlow in 1909,[2] many models have described the variation of the melting temperature with the particle size.[3–16] This behavior is explained by the particular role played by the surface at the nanoscale. Indeed, when the size decreases, the number of atoms at the surface is no longer negligible compared to the number of atoms in the (bulk) volume. To study the melting temperature at the nanoscale, there are two approaches currently used: bottom up and top down. The first makes use of computational methods such as molecular dynamics, whereas the second relies on classical thermodynamics. Molecular dynamics generally considers less than 10^5 atoms in order to keep calculation times within reasonable values. This factor limits the nanostructure size modeled to a maximum size of tens of nanometers, but, on the other hand, effects such as chemical environment on the melting temperature can be considered. Therefore, the top-down approach, wherein one can consider bigger particles ($R>2$ nm), emerges as a simple complementary method that may provide useful insights in nanotechnology.

Here, we adopt the top-down approach using classical thermodynamics. The melting temperature at the nanoscale T_m for freestanding nanostructures can be expressed as a function of the bulk melting temperature $T_{m,\infty}$, the size of the structure, and some material properties,[11]

$$\frac{T_m}{T_{m,\infty}} = 1 + \frac{(\gamma_l - \gamma_s)}{\Delta H_{m,\infty}} \frac{A}{V}, \tag{1}$$

where $\Delta H_{m,\infty}$ is the melting enthalpy (J/m^3) and γ_l and γ_s are the surface energy in the liquid and solid phases (J/m^2),

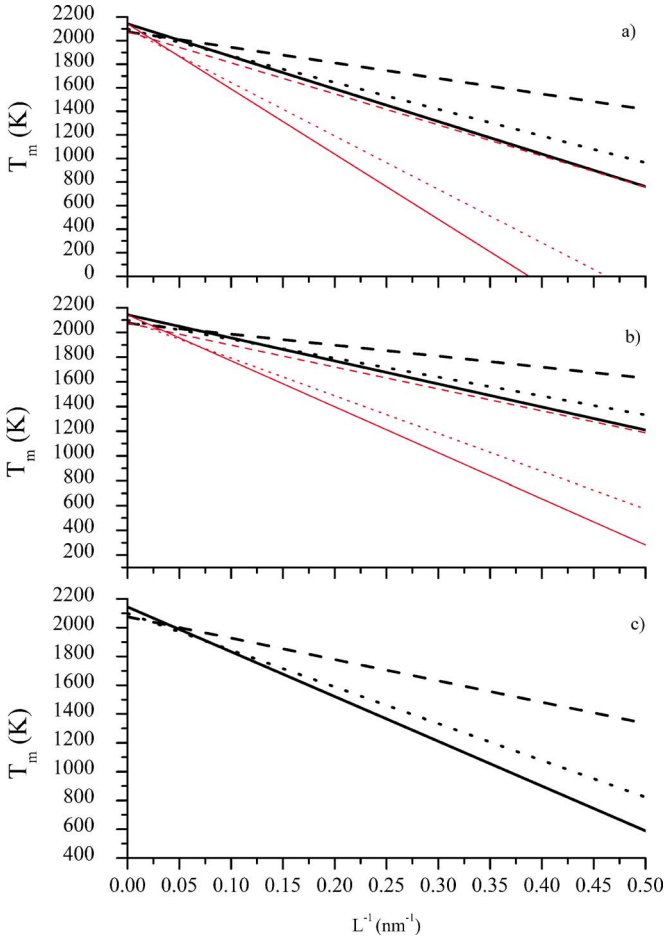

FIG. 1. (Color online) Melting temperature vs the reciprocal size for (a) spherical and cubic TiO_2 nanoparticles, (b) cylindrical and parallelepipedic TiO_2 nanowires with a length of 100 nm, and (c) cylindrical TiO_2 nanotubes with a length of 100 nm and a ratio of the outer to inner diameter equals 1.6. The solid, dashed, and dotted lines represent the rutile, anatase, and brookite phases, respectively. The thick black lines represent the nanostructures with a circular section, and the thin red lines represent the nanostructures with a square section.

[a]Author to whom correspondence should be addressed. Present address: Physics of Condensed Matter, University of Mons-Hainaut, 23 Avenue Maistriau, 7000 Mons, Belgium. Electronic mail: gregory.guisbiers@physics.org

TABLE I. Bulk material properties of different phases of TiO_2 (Refs. 21, 22, and 30–32).

Phase	$T_{m,\infty}$ (K)	γ_l (J m^{-2})	γ_s (J m^{-2})	$\Delta H_{m,\infty}$ (10^9 J m^{-3})	E_g (eV)
Rutile	2143		1.91	3.5585	3.05
Anatase	2075	0.38	1.32	4.4426	3.23
Brookite	2098		1.66	3.5532	3.26

respectively. A (m^2) and V (m^3) are the surface area and volume of the nanostructure, respectively. To describe the size effect with only one parameter, let us rewrite Eq. (1) more conveniently as[11,17]

$$\frac{T_m}{T_{m,\infty}} = 1 - \frac{\alpha_{\text{shape}}}{2L}, \tag{2}$$

where the shape parameter α_{shape} is defined as $\alpha_{\text{shape}} = 2AL(\gamma_s - \gamma_l)/(V\Delta H_{m,\infty})$, where L is the smallest dimension of the structure (i.e., for a sphere, $L=R$).

One should note that thermodynamics, as a phenomenological theory, is strictly valid for macroscopic systems; therefore, it is necessary to obtain a statistical limit of validity in terms of size in classical thermodynamics. Considering that the relative temperature fluctuation inside a cube $\delta T/T \approx (nL^3)^{-1/2}$ (where L^3 is the volume of the cube with n atoms per unit volume) is less than 1% for $L \geqslant 5$ nm and ~3% for $L \approx 2$ nm, the size limit we consider for the application of thermodynamics is ~2 nm. This is the lower size limit that we will use in this work. Therefore, any shape instability effects due to the thermal fluctuations above 3% are not addressed here, and other methods such as molecular dynamics simulations should be considered for such extremely small nanostructures (<2 nm) or clusters of atoms.[13–15,18]

This theory can now be applied to the particular case of TiO_2 nanostructures. The magnitudes of size effects on the melting temperature are shown on Fig. 1 for different shapes of TiO_2 nanostructures. The basic material parameters considered are summarized in Table I, and the values used for α_{shape} are indicated in Table II. In Table II, the ratio R_1/R_2 (=1.6) defining the wall thickness of the nanotubes has been chosen according to the experimental data reported by Yuan and Su.[19] Within this thermodynamical approach, we predict a structural phase transition from rutile to anatase for a size (=2R) around 40 nm in the case of spherical nanoparticles. This means that the more stable phase is anatase for sizes smaller than ~40 nm and rutile for sizes larger than ~40 nm. At room temperature (~300 K), the TiO_2 spherical nanoparticles are rutile for $R > 1.5$ nm, brookite for 1.5 nm $> R > 1.3$ nm, and anatase for $R > 1.3$ nm. At 1000 K, the TiO_2 spherical nanoparticles are rutile for $R > 2.4$ nm, brookite for 2.4nm $> R > 2.1$ nm, and anatase for $R < 2.1$ nm. Among the three phases (rutile, anatase, and brookite), the preferential adopted phase corresponds to the highest melting temperature because it minimizes the Gibbs free energy. As noted by Reddy *et al.*,[20] the brookite phase is only stable at low temperatures. This behavior can be seen in Fig. 1. Therefore, from Fig. 1, we consider only the rutile and anatase phases as stable. The structural phase transitions are temperature and size dependent. These results can be compared with the size of ~8–15 nm announced by Zhang and Banfield[21,22] for the rutile-anatase phase transition for the temperature range between 300 and 1000 K. The increase in temperature increases the size at which the structural phase transition occurs; the same trend was also noted by Zhang and Banfield.

In the case of TiO_2 cylindrical nanowires and nanotubes (with a length of 100 nm), we predict a structural phase transition from rutile to anatase for sizes (=2R) around 29 and 48 nm, respectively.

Note that our calculations consider an isotropic value for the solid surface energy γ_s. Therefore, let us estimate the error on the nanoscale melting temperature calculated with isotropic and anisotropic values.[21] For spherical nanoparticles and cylindrical nanowires, the error is less than 7% (3%) and 5% (2%) of the TiO_2 bulk melting temperature in the case of the rutile (anatase) phase. Furthermore, we do not consider the effects of the diverse chemical environments that may be used in the growth or synthesis of TiO_2 nanostructures. Considering the surface energy $\gamma_s(hkl)$ of each crystal face (hkl) and the influence of the chemical environment on the surface energy of the crystal faces, it is not surprising that the other shapes may certainly appear experimentally. With a suitable tuning of the chemical environment of the nanostructures, it is possible to favor the growth of one particular shape over another because we can decrease the surface energy relative to the isotropic value γ_s.

The energy bandgap is well known to be temperature dependent.[23] The energy bandgap of semiconductors tends to increase as the temperature is decreased. This behavior can be better understood if one considers that the interatomic spacing decreases when the amplitude of the atomic vibrations decreases due to the decreased thermal energy. A decreased interatomic spacing increases the potential seen by the electrons in the material, which, in turn, increases the size of the energy bandgap. Therefore, such temperature-dependent property is also size dependent due to the size effect on the melting temperature. It means that with the same α_{shape} parameter, we can describe the size effect on the energy bandgap of semiconductors with the following equation:[24,25]

TABLE II. α_{shape} parameters for different shapes of TiO_2 nanostructures.

		Nanoparticle		Nanowire with different section (h=100 nm)		Nanotube (h=100 nm)
	Phase\section	Sphere	Cube	Circle	Square	Circle (R_1/R_2=1.6)
α_{shape} (nm)	Rutile	2.58	5.16	1.74	3.47	2.90
	Anatase	1.27	2.54	0.86	1.71	1.43
	Brookite	2.16	4.32	1.46	2.91	2.43

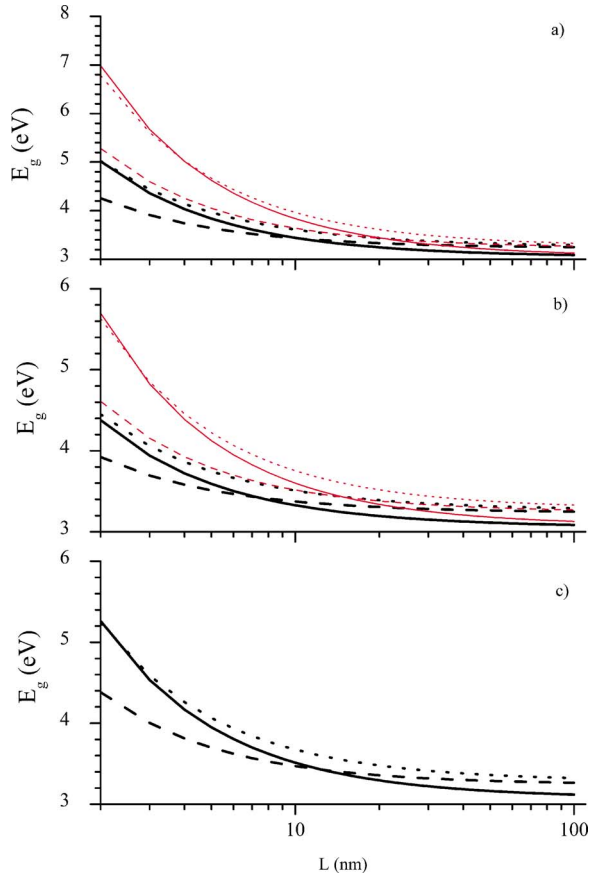

FIG. 2. (Color online) Bandgap vs the size for (a) spherical and cubic TiO_2 nanoparticles, (b) cylindrical and parallelepipedic TiO_2 nanowires with a length of 100 nm, and (c) cylindrical TiO_2 nanotubes with a length of 100 nm and a ratio of the outer to inner diameter equals 1.6. The solid, dashed, and dotted lines represent the rutile, anatase, and brookite phases, respectively. The thick black lines represent the nanostructures with a circular section, and the thin red lines represent the nanostructures with a square section.

$$\frac{E_g - E_{g,\infty}}{E_{g,\infty}} = 1 - \frac{T_m}{T_{m,\infty}}. \quad (3)$$

This means that for freestanding nanostructures, as the melting temperature decreases with the size, the energy bandgap increases with the size. This is illustrated in Fig. 2 for the three different phases of TiO_2. Considering a spherical section for TiO_2 nanoparticles, nanowires, and nanotubes, α_{nanowire} has the lowest value; therefore, a TiO_2 nanowire has a bandgap lower than those of TiO_2 nanoparticles and nanotubes. On the contrary, α_{nanotube} is higher, and then this structure is characterized by a higher bandgap. As the Bohr radius of TiO_2 is 1.5 nm,[26] the quantum confinement in the structures considered in this paper is weak.

Quantitatively, these results can be compared to the value of the energy bandgap announced by Reddy *et al.*[20] in the case of anatase TiO_2 spherical nanoparticles. They calculated $\Delta E_g \approx 0.2$ eV for a size of 10 nm. In this work, we predict the same order of magnitude, $\Delta E_g \approx 0.4$ eV. The bandgap and melting temperature differences observed between experimental results and our predictions can be explained by considering the anisotropy of surface energy and also the size effect on the surface energy[27] and melting enthalpy.[28,29]

In this letter, we have investigated the structural phase transitions which occur in TiO_2 nanostructures. From the same thermodynamic approach, the energy bandgap is also estimated; therefore, the same α_{shape} parameter can be used to calculate the size effect on the melting temperature and the energy bandgap. This approach can be applied to other semiconductors.

Grégory Guisbiers would like to acknowledge financial support from Fundação para a Ciência e Tecnologia (FCT). Grégory Guisbiers is being funded by an FCT postdoctoral grant (SFRH/BPD/34727/2007).

[1] O. Carp, C. L. Huisman, and A. Reller, Prog. Solid State Chem. **32**, 33 (2004).
[2] P. Pawlow, Z. Phys. Chem., Stoechiom. Verwandtschaftsl. **65**, 1 (1909).
[3] J. P. Borel, Surf. Sci. **106**, 1 (1981).
[4] A. N. Goldstein, C. M. Echer, and A. P. Alivisatos, Science **256**, 1425 (1992).
[5] K. K. Nanda, S. N. Sahu, and S. N. Behera, Phys. Rev. A **66**, 013208 (2002).
[6] C. Q. Sun, Prog. Solid State Chem. **35**, 1 (2007).
[7] P. Buffat and J. P. Borel, Phys. Rev. A **13**, 2287 (1976).
[8] A. Safaei, M. A. Shandiz, S. Sanjabi, and Z. H. Barber, J. Phys.: Condens. Matter **19**, 216216 (2007).
[9] C. Q. Sun, B. K. Tay, X. T. Zeng, S. Li, T. P. Chen, J. Zhou, H. L. Bai, and E. Y. Jiang, J. Phys.: Condens. Matter **14**, 7781 (2002).
[10] M. Wautelet, J. Phys. D **24**, 343 (1991).
[11] M. Wautelet, Phys. Lett. A **246**, 341 (1998).
[12] Z. Zhang, M. Zhao, and Q. Jiang, Semicond. Sci. Technol. **16**, L33 (2001).
[13] G. Guisbiers and M. Wautelet, Nanotechnology **17**, 2008 (2006).
[14] G. Abudukelimu, G. Guisbiers, and M. Wautelet, J. Mater. Res. **21**, 2829 (2006).
[15] G. Guisbiers, G. Abudukelimu, F. Clements, and M. Wautelet, J. Comput. Theor. Nanosci. **4**, 309 (2007).
[16] G. Guisbiers, M. Kazan, O. Van Overschelde, M. Wautelet, and S. Pereira, J. Phys. Chem. C (to be published), doi: 10.1021/jp077371n.
[17] G. Guisbiers and S. Pereira, Nanotechnology **18**, 435710 (2007).
[18] M. Wautelet and D. Duvivier, Eur. J. Phys. **28**, 953 (2007).
[19] Z. Y. Yuan and B. L. Su, Colloids Surf., A **241**, 173 (2004).
[20] K. M. Reddy, S. V. Manorama, and A. R. Reddy, Mater. Chem. Phys. **78**, 239 (2003).
[21] H. Z. Zhang and J. F. Banfield, J. Mater. Chem. **8**, 2073 (1998).
[22] H. Z. Zhang and J. F. Banfield, J. Phys. Chem. B **104**, 3481 (2000).
[23] S. P. Keller, *Handbook on Semiconductors: Materials, Properties and Preparation* (North-Holland, Amsterdam, 1980), Vol. 3.
[24] M. Li and J. C. Li, Mater. Lett. **60**, 2526 (2006).
[25] C. C. Yang and Q. Jiang, Mater. Sci. Eng., B **131**, 191 (2006).
[26] D. C. Pan, N. N. Zhao, Q. Wang, S. C. Jiang, X. L. Ji, and L. J. An, Adv. Mater. (Weinheim, Ger.) **17**, 1991 (2005).
[27] R. C. Tolman, J. Chem. Phys. **17**, 333 (1949).
[28] L. H. Liang, M. Zhao, and Q. Jiang, J. Mater. Sci. Lett. **21**, 1843 (2002).
[29] Z. Zhang, X. X. Lu, and Q. Jiang, Physica B **270**, 249 (1999).
[30] Y. L. Li and T. Ishigaki, J. Cryst. Growth **242**, 511 (2002).
[31] W. Martienssen and H. Warlimont, *Springer Handbook of Condensed Matter and Materials Data* (Springer, Berlin, 2005).
[32] K. Shankar, M. Paulose, G. K. Mor, O. K. Varghese, and C. A. Grimes, J. Phys. D **38**, 3543 (2005).